A simple and sensitive aptasensor for colorimetric detection of adenosine triphosphate based on unmodified gold nanoparticles

Yu Mao, Tingting Fan, Rachel Gysbers, Yin Tan, Feng Liu, Shuo Lin, Yuyang Jiang

www.elsevier.com/locate/talanta

PII: S0039-9140(17)30289-8
DOI: http://dx.doi.org/10.1016/j.talanta.2017.03.014
Reference: TAL17359

To appear in: *Talanta*

Received date: 17 December 2016
Revised date: 28 February 2017
Accepted date: 2 March 2017

Cite this article as: Yu Mao, Tingting Fan, Rachel Gysbers, Yin Tan, Feng Liu, Shuo Lin and Yuyang Jiang, A simple and sensitive aptasensor for colorimetric detection of adenosine triphosphate based on unmodified gold nanoparticles *Talanta,* http://dx.doi.org/10.1016/j.talanta.2017.03.014

A simple and sensitive aptasensor for colorimetric detection of adenosine triphosphate based on unmodified gold nanoparticles

Yu Mao[a,b], Tingting Fan[b], Rachel Gysbers[c], Yin Tan[b], Feng Liu[b], Shuo Lin[a,d], Yuyang Jiang[b]*

[a]Laboratory of Chemical Genomics, School of Chemical Biology and Biotechnology, Peking University Shenzhen Graduate School, Shenzhen 518055, China

[b]The Ministry-Province Jointly Constructed Base for State Key Lab-Shenzhen Key Laboratory of Chemical Biology, the Graduate School at Shenzhen, Tsinghua University, Shenzhen 518055, China

[c]Department of Biochemistry and Biomedical Sciences, McMaster University, 1280 Main St. W., Hamilton, ON L8S 4K1, Canada

[d]Department of Molecular, Cell and Developmental Biology, University of California, Los Angeles, CA 90095, United States

*Correspondence should be addressed. Tel./Fax: +86 755 2603 2094. E-Mail: jiangyy@sz.tsinghua.edu.cn

Abstract

A simple and sensitive colorimetric aptasensor for rapid and facile detection of adenosine triphosphate (ATP) has been demonstrated here based on aptamer-based hairpin probes and unmodified gold nanoparticles (AuNPs). The hairpin probe is constructed by adding another five nucleotides to the 5'-end of an anti-ATP aptamer which can hybridize to nucleotides at the 3'-end of the aptamer, forming a hairpin-shaped structure. In the absence of ATP, the hairpin probes are rigid, and the AuNPs are susceptible to salt-induced aggregation. Conversely, upon binding with target ATP, the hairpin probes undergo conformational changes, forming aptamer-ATP complexes and exposing flexible ends which coat the surface of AuNPs to inhibit their aggregation in the high salt solution. Subsequently, a blue-to-red color change can be recognized by the naked eye. The aptasensor achieved selective responses toward ATP with a detection limit of 0.1 μM, and exhibited high-quality detection performance in biological samples. In addition, this detection method is simple, rapid and cost-effective, holding great potential for further applications in point-of-care research.

Graphical Abstract

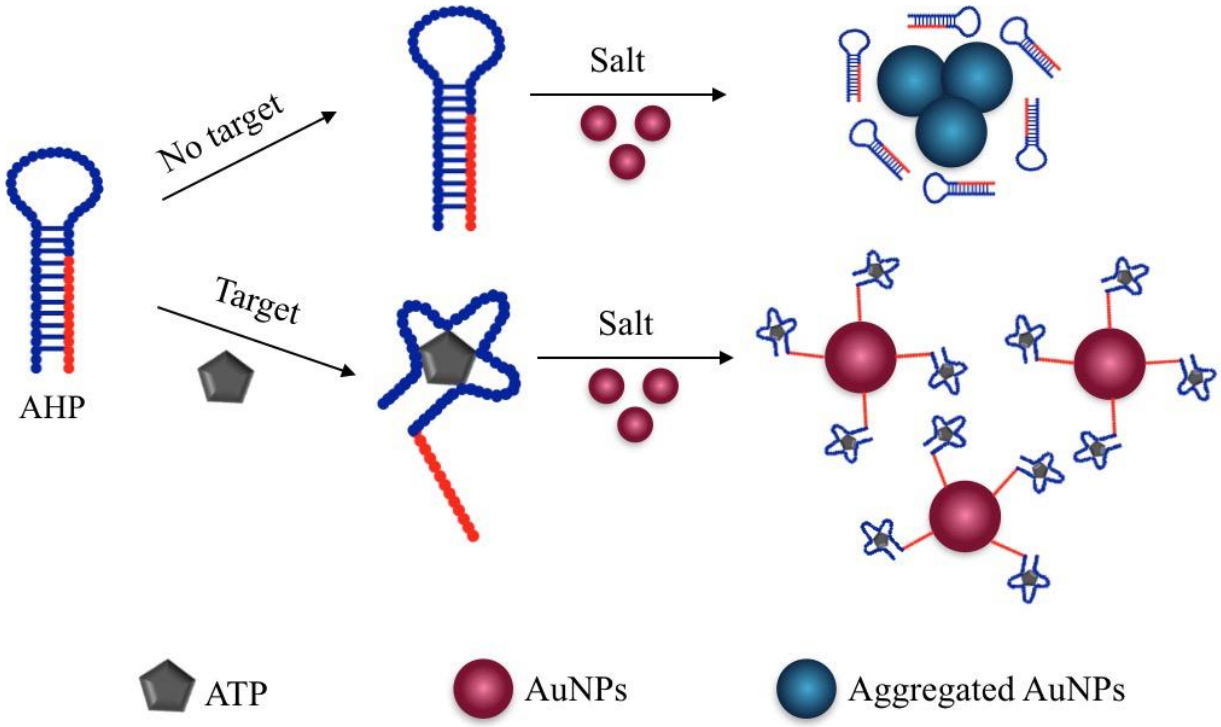

The principle of the proposed strategy for colorimetric detection of ATP using unmodified gold nanoparticles is shown in the above graph. The aptamer-based hairpin probe (AHP) was constructed with anti-ATP aptamer (blue region) and another five nucleotides (red region) added to the 5'-end of the aptamer which were complementary to nucleotides at the 3'-end of the aptamer, forming a hairpin-shaped structure. In the absence of ATP, the hairpin probes were rigid, and their negatively charged phosphate backbones were exposed. The strong repulsion between the hairpin probes and negatively charged AuNPs made their binding negligible, which could not prevent salt-induced AuNP aggregation. Conversely, in the presence of ATP, the hairpin probes under went a conformational change, forming aptamer-ATP complexes and exposing flexible ssDNA ends (red region). The ssDNA ends had strong attractive electrostatic interactions with AuNPs and thus prevented them from salt-induced aggregation, corresponding to a blue-to-red colour change and thus providing the colorimetric detection of the target ATP.

Keywords: biosensor; aptamer; gold nanoparticles; colorimetric detection.

1. Introduction

Aptamers are functional nucleic acids obtained from random-sequence DNA or RNA libraries using in vitro selection techniques [1, 2].They possess highly specific molecular recognition capabilities toward a vast range of targets, including small molecules [3, 4], metal ions [5], proteins [6, 7], and even cells [8, 9].In recent years, aptamers have been extensively applied as recognition elements for biosensor design due to their high selectivity and affinity [10-12]. Moreover, they have the advantages of simple synthesis, easy modification, excellent stability, and high flexibility. Thus, they can serve as promising candidates for biosensors.

Aptamer-based biosensors have attracted substantial research efforts due to their high sensitivity and selectivity. The majority of these sensors are based on fluorescence [13-19], electrochemistry [20-23], chemiluminescence [24-26]and colorimetry [27-31]. Among these detection strategies, aptamer-based colorimetric methods have been commonly applied for routine analysis and are attracting more and more attention because of their relatively low cost, simplicity and easy read-out.

To successfully develop a valuable colorimetric assay, the use of signal indicators is very crucial to achieve a high sensitivity and efficiency. Gold nanoparticles (AuNPs) have been demonstrated to be highly competitive for colorimetric analysis based on their high extinction coefficients, strong distance dependent optical properties, unique size, low cost and simplicity [32-35]. There are two major classes of AuNP-based colorimetric assays. The first class utilizes a three-component sandwich assay format. In this assay, the AuNP aggregation is induced by an interparticle cross-linking mechanism where AuNPs are modified with thiolated oligonucleotide probes [36-38]. The second class of the colorimetric assay relies on the difference in binding properties of single-stranded DNA (ssDNA) and double-stranded DNA (dsDNA) or folded DNA toward unmodified AuNPs [32, 39]. The ssDNA is flexible and can uncoil its bases, bind to unmodified AuNPs and effectively inhibit their aggregation in high salt solution. On the other hand, dsDNA or folded DNA is stiffer and does not permit uncoiling, which means that the AuNPs are inclined towards salt-induced aggregation. The second strategy has been paid more and more attention since it does not require complicated and time-consuming steps, such as surface modification and separation. Based on the principle, a number of aptamer-based colorimetric sensors using unmodified AuNPs have been developed [32, 40-44]. Aptamers are widely

used as ligands to bind target molecules and resulting in conformational change which can be discriminated by the color change of unmodified AuNPs [42, 45]. However, not all aptamers exhibit obvious conformational changes upon binding. As an alternative strategy, aptamers are initially hybridized to their complementary sequences, forming a rigid duplex. The binding with target molecules dissembles the original duplex and release ssDNA sequences. This disassembly process can be discerned by the color change of AuNPs [21, 46]. However, this strategy is usually time-consuming. Recent studies have discovered that some target molecules can bind to their aptamers, forming target-aptamer complexes which bind to and protect AuNPs against salt-induced aggregation more efficiently than target and aptamer alone [29]. However, the aptamer itself can bind to AuNPs and result in a background signal. The generalizability of this strategy is limited because of the different properties of various aptamers. Thus, it is important to find new strategies that can overcome these problems.

Adenosine triphosphate (ATP), as an intracellular energy carrier, plays a critical role in the metabolic processes for daily activities. It has been found that ATP is an indicator for cell viability and cell injury [47]. The concentration of ATP is closely related to many diseases such as angiocardiopathy [48], Parkinson's disease [49] and malignant tumors [50]. Therefore, the detection of ATP is of great value in biochemical studies and clinic diagnosis.

Herein, we report on a novel colorimetric aptasensor for the detection of ATP by coupling an aptamer-based hairpin probe (AHP) with visible-colored unmodified AuNPs. The hairpin probe is constructed by adding an additional five nucleotides to the 5’-end of an anti-ATP aptamer which are complementary to nucleotides at the 3’-end of the aptamer. In the absence of ATP, the hairpin probes are rigid, and cannot prevent AuNPs against salt-induced aggregation. Upon binding with target ATP, the hairpin probes undergo a conformational change, forming aptamer-ATP complexes and exposing flexible ends. The flexible ends can coat on AuNPs and thus prevent them from salt-induced aggregation. As a result, a blue-to-red colour change can be observed. In this case, the detection can be carried out based on the change in color by using the naked eye and without a need for sophisticated instruments. Moreover, the aptasensor is simple in design, convenient for use and can be adapted for carrying out on-site measurements.

2. Experimental Section

2.1. Materials and Chemicals

AHP (5'-ACCTTCCTGGGGGAGTATTGCGGAGGAAGGT-3') was synthesized and purified with HPLC by Sangon Biotech Company, Ltd (Shanghai, China). The stock solution of AHP was prepared by dissolving the lyophilized powder in 20 mM Tris–HCl buffer (100 mM NaCl, 5 mM $MgCl_2$, pH 7.4). The AHP solution was heated to 95 °C for 5 min and then allowed to cool down to room temperature to form designed hairpin structure before use. Adenine (A), thymine (T), guanine (G) and cytosine (C) were obtained from Takara Biotechnology Co. Ltd. (Dalian, China). Chloroauric acid ($HAuCl_4.4H_2O$) and sodium citrate were obtained from Sinopharm Chemical Reagent Co., Ltd (Shanghai, China). All other reagents were of analytical grade and used as received. Ultrapure water obtained from a Millipore water purification system (Milli-Q, Millipore) was used for all experiments.

2.2. Apparatus

Absorbance measurements were recorded with a microplate reader (Tecan infinite M1000 Pro, Männedorf, Switzerland). The absorption spectra of the solution were collected from 400 to 800 nm with a step of 2 nm. Transmission electron microscopy (TEM) measurements were made on Tecnai G2 Spirit120kV with an accelerating voltage of 120 kV. The samples for TEM characterization were prepared by placing a drop of colloidal solution on carbon-coated copper grid and dried at room temperature.

2.3. Preparation of Gold Nanoparticles

Gold nanoparticles (~14 nm) were first prepared by the citrate reduction of $HAuCl_4$ [51]. In a typical experiment, a 5 mL aqueous solution of sodium citrate (1 wt %) was added to a boiling solution of $HAuCl_4$ (50 mL, 1 mM). The reaction mixture was allowed to reflux for another 20 min after the color of the solution changed to red. The solution was then cooled down in ice and stored in a refrigerator at 4 °C before use. The concentration of the AuNPs was estimated to 10 nM, using Beer's law [$A=\varepsilon lc$, where the extinction coefficient (ε) is calculated by the equation ($\ln \varepsilon=1.4418\times\ln D+18.955$), D is the diameter in nm] [52].

2.4. Cell Culture and Cell Lysate Preparation

The adherent breast cancer cell line MCF-7 was cultured in DMEM media (Corning) and supplemented with 10% fetal bovine serum (Biochrom). Cell cultures were incubated at 37 °C in a humidified incubator maintained at 5% CO_2. Cell lysates were prepared by the following method. Cells were grown to approximately 80% confluence before harvesting. Then the media was removed, and cells were washed with PBS. Cells were coated with 1 mL trypsin-EDTA solution (0.25% trypsin, 0.02% EDTA, Beyotime) and the excess was removed. Cells were incubated at 37 °C for 3 min to dissociate cells. Dissociated cells were

suspended in 1 mL of PBS and pelleted by centrifugation at 3000 g for 5 min. Supernatant was removed, and cell pellet was resuspended in 1 mL of 20 mM Tris-HCl buffer (100 mM NaCl, 5 mM $MgCl_2$, pH7.4) and EDTA-free protease inhibitor cocktail (Sigma) was added to the cell suspension at 1 final concentration. The cells were lysed by Ultrasonic Cell Disruption System (Misonix) for 10 times. Then the solution was centrifuged at 14000 rpm for 10 min at 4°C. The supernatant was collected and a fraction of it was taken for cell counting to ensure complete lysis.

2.5. Measurement Procedure

In a typical target ATP assay, different concentrations of ATP were mixed with AHP (1 μM) in 20 mM Tris–HCl buffer (100 mM NaCl, 5 mM $MgCl_2$, pH 7.4) and incubated for 5 min. Subsequently, 10 μL of the above-mentioned reaction mixture was added into 190 μL AuNP solution (2.5 nM). Finally, 5 μL of 1 M sodium chloride solution was rapidly added, and the mixed solution was detected by either visual observation or UV–vis absorption spectrum. All processes were conducted at room temperature.

3. Results and Discussion

3.1. Principle of the Colorimetric Assay

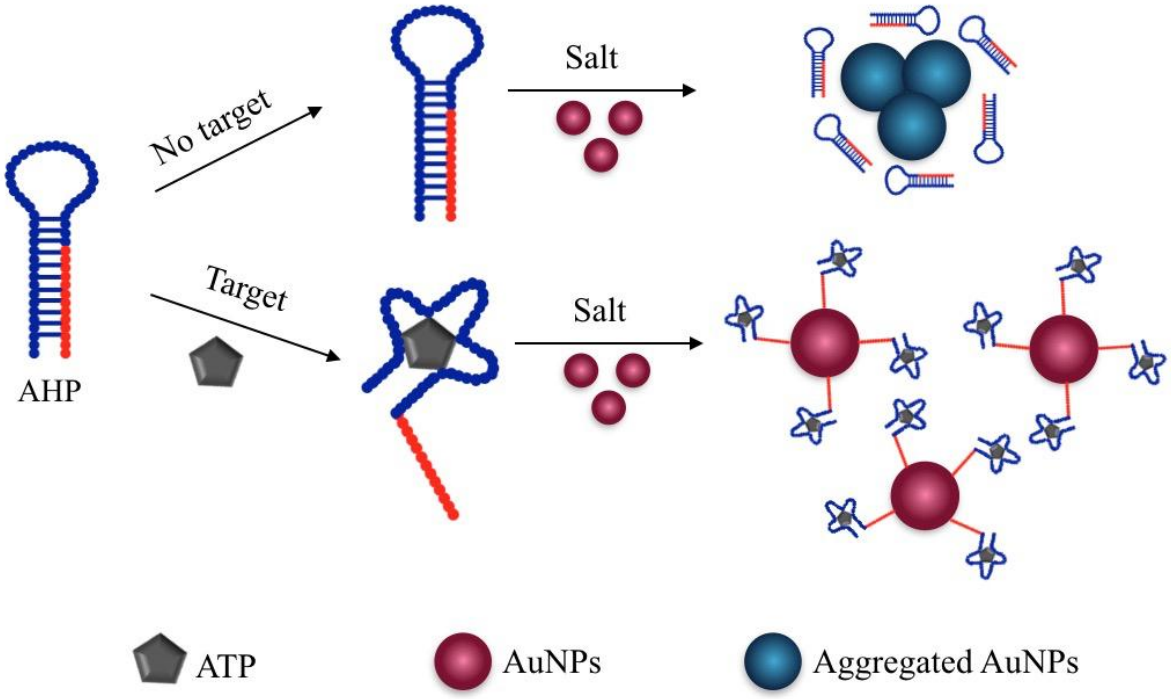

Fig. 1. Schematic illustration of ATP detection based on colorimetric assay. In the absence of target ATP,

the aptamer-based hairpin probe (AHP) could not prevent salt-induced AuNP aggregation, leading to an observation of blue color. In the presence of target ATP, the hairpin-shaped probe undergoes a conformational change, forming aptamer-ATP complex and exposing flexible end. The flexible end can coat on AuNPs and thus prevent them from salt-induced aggregation, resulting in a red color.

The principle of the proposed strategy for colorimetric detection of ATP using unmodified gold nanoparticles is shown in Fig. 1. The aptamer-based hairpin probe (AHP) was constructed with anti-ATP aptamer (blue region) and another five nucleotides (red region) added to the 5'-end of the aptamer which were complementary to nucleotides at the 3'-end of the aptamer, forming a hairpin-shaped structure. In the absence of ATP, the hairpin probes were rigid, and their negatively charged phosphate backbones were exposed. The strong repulsion between the hairpin probes and negatively charged AuNPs made their binding negligible, which could not prevent salt-induced AuNP aggregation. Conversely, in the presence of ATP, the hairpin probes underwent a conformational change, forming aptamer-ATP complexes and exposing flexible ssDNA ends (red region). The ssDNA ends have strong attractive electrostatic interactions with AuNPs and thus prevented them from salt-induced aggregation, corresponding to a blue-to-red colour change and thus providing the colorimetric detection of the target ATP.

3.2. Investigation of the Feasibility and Mechanism of the Aptasensor

In order to investigate the feasibility and mechanism of the aptasensor, AuNPs solutions with different biomolecules were prepared: blank with salt (sample a); ATP with salt (sample b); AHP in the absence of ATP with salt (sample c); and AHP in the presence of target ATP with salt (sample d). Fig.2 shows UV−vis absorption spectra and the corresponding photographs of AuNP solutions. As shown in Fig. 2, sample a, sample b and sample c exhibited a surface plasmon resonance absorption peak at approximately 656 nm, and the color of the solution appeared blue. However, a distinctive absorption peak at 522 nm was observed for sample d, and the color of the solution maintained red. These phenomena indicated that the hairpin probe and ATP itself could not prevent the AuNPs from aggregation in the presence of salt. While in the presence of target ATP, the hairpin probes underwent conformational change, forming aptamer-ATP complexes and exposing flexible ssDNA ends which could protect AuNPs from aggregation in the high salt solution. These results were consistent with the proposed mechanism shown in Fig 1.

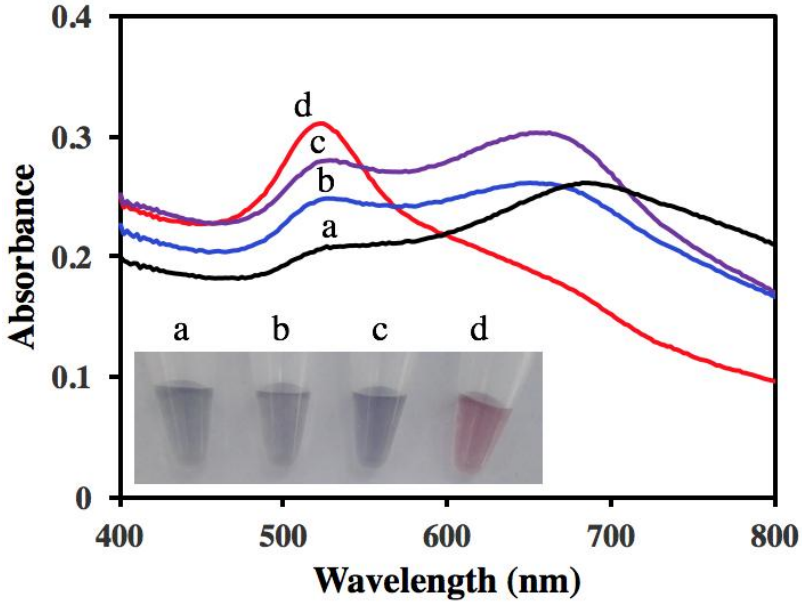

Fig.2. UV–vis absorption spectra of AuNPs solution with (a) salt, (b) ATP+salt, (c) AHP+salt, (d) ATP+AHP+salt, respectively (Inset: the corresponding photographs) (Note: 2.5 nM AuNPs, 1 μM AHP, 10 μM ATP and 25 mM salt were used in these cases).

To show the changes in AuNPs morphology, AuNPs with AHP in the absence or in the presence of target ATP were further characterized using transmission electron microscopy (TEM). The corresponding TEM images of AuNPs were shown in Fig. 3. As shown, AuNPs aggregated heavily in the absence of target ATP (Fig. 3A). While in the presence of the target ATP, the AuNPs were well-dispersed (Fig. 3B). The TEM results were consistent with the UV–vis absorption spectra as well as the color change of AuNPs solution.

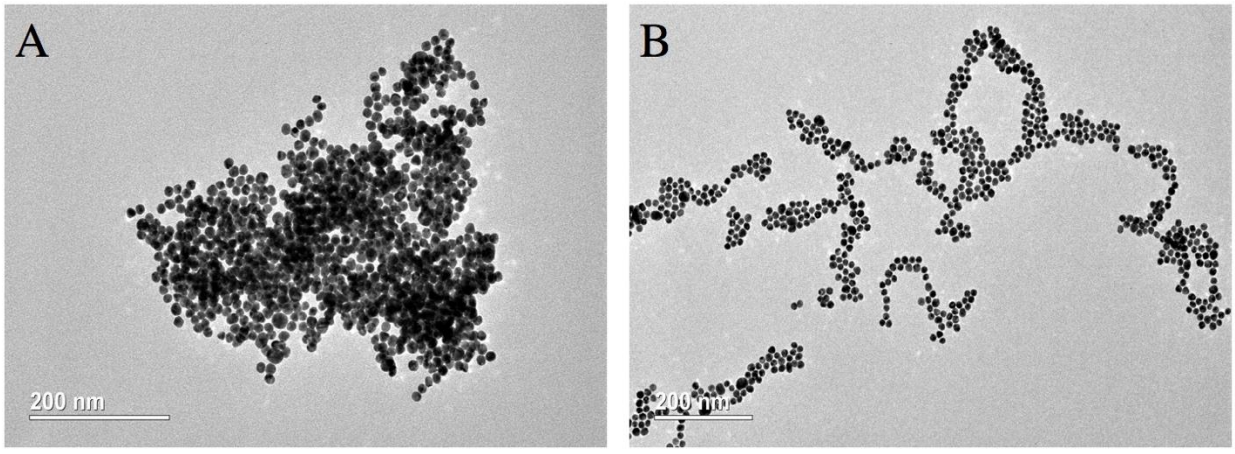

Fig. 3. TEM images of the 2.5 nM AuNPs solution mixed with (A) AHP+salt, and (B) ATP+AHP+salt.

3.3. Optimization of Detection Conditions

According to the detection principle, experimental conditions such as the amount of AHP, the concentration of salt, the concentration of AuNPs and incubation time have a great effect on the sensitivity of the colorimetric method. Hence, a series of systematic optimization experiments were carried out to obtain the optimal assay conditions. Since the absorption ratio between 522 nm and 656 nm (A_{522}/A_{656}) is associated with the aggregation state of AuNPs, with a low ratio corresponding to high degree of AuNPs aggregation. The odds ratio (OR) between 680 nm and 520 nm, ORA_{522}/A_{656} (ORA_{522}/A_{656}= [the A_{522}/A_{656} absorption ratio in the presence of ATP] / [the A_{522}/A_{656}absorption ratio in the absence of ATP]), was used to optimize the experimental conditions. Firstly, the effect of the AHP amount on the assay performance was investigated (0.1-2 μM range). As shown in Fig. 4A, the ORA_{522}/A_{656} reached a maximum value at 1 μM AHP. Thus, subsequent work employed 1 μM of AHP. Next, the effect of salt concentration was examined (20-40 mM range). The result showed that maximal ORA_{522}/A_{656} value was obtained at 35 mM Salt (Fig. 4B). Therefore, 35 mM salt was selected for the following experiments. The effect of AuNPs concentration was also investigated (1.5-3.5 nM range). As shown in Fig. 4C, the highest value of ORA_{522}/A_{656} was observed at 2nMAuNPs. Hence, an AuNPs concentration of 2 nM was selected for further study. Finally, we investigated the effect of incubation time on the detection. The results in Fig. 4Ddemonstrated that 5 min is enough to induce the conformational change of AHP in the presence of ATP. To optimize the assay time, 5 min was used in the later experiments.

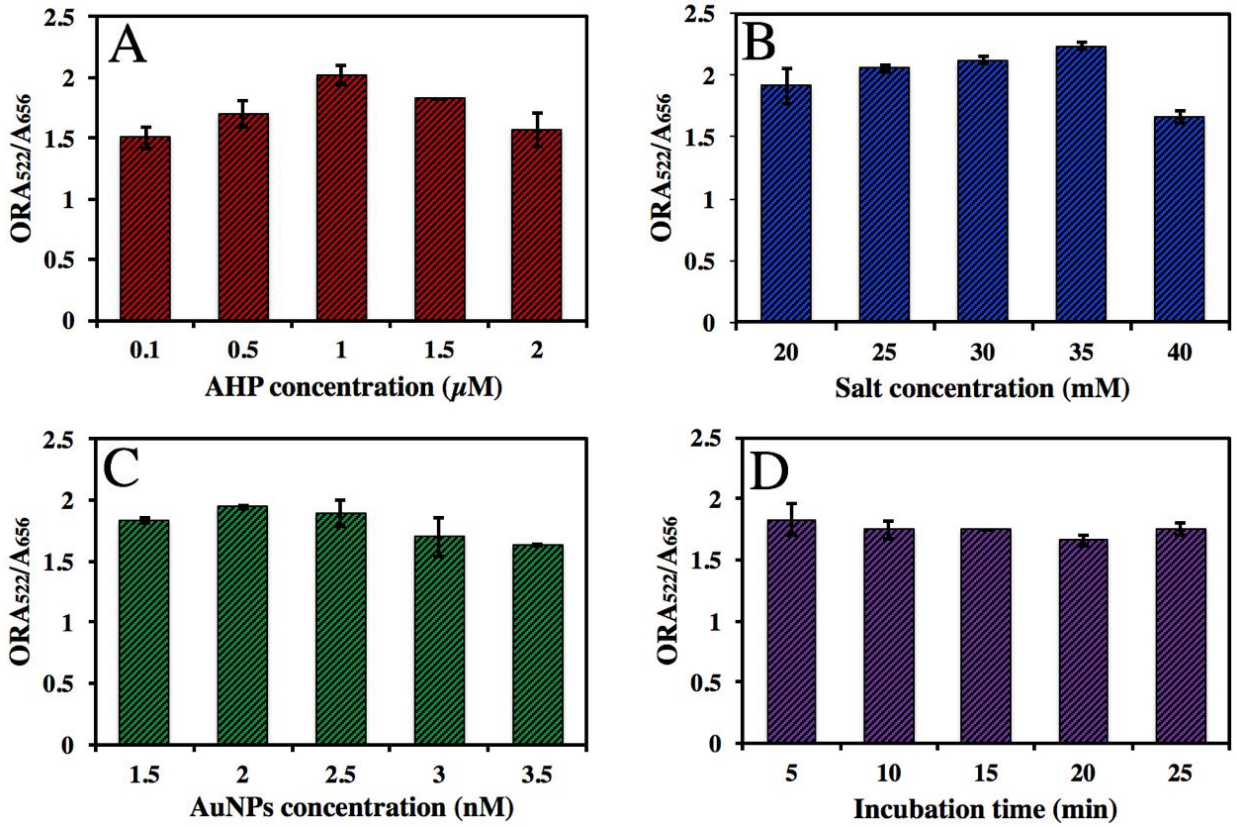

Fig. 4. Dependence of the odds ratio of absorbance (A_{522}/A_{656}) on (A) AHP concentration, (B) salt concentration, (C) AuNPs concentration, and (D) incubation time (Note: 10 μM ATP was used in these cases). Error bars: SD, n=3.

3.4. Sensitivity for ATP Detection

Under the optimal conditions, the aptamer-based colorimetric assay was employed for the quantitative monitoring of target ATP by UV–vis spectroscopy. The absorption ratio between 522 nm and 656 nm (A_{522}/A_{656}) profiles and the color change of the AuNPs with different concentration of target DNA were measured. As shown in Fig. 5A, in the absence of ATP, the AHP was ineffective in protecting the AuNPs against salt-induced aggregation, and thus a blue color of the aggregated AuNPs was observed. As expected, in the presence of ATP, ATP bound to the aptamer region in AHP, exposing flexible ssDNA ends which could coat on the surface of AuNPs to inhibit their aggregation in the high salt solution, resulting in different extents of AuNPs aggregation and thus different colors (blue to red). Fig. 5B gives UV–vis absorption spectra of the AHP-AuNP system toward target ATP with different concentrations. Upon the addition of target ATP, an observable aggregation phenomenon of AuNPs appeared with an increase of the absorbance at 522 nm and a decrease of the absorbance at 656 nm. In addition, A_{522}/A_{656} continued to decrease with the increase in ATP concentration until

reaching a plateau (Fig. 5C). The absorption ratio of AuNPs showed good linear correlation to target ATP concentration within the range from 0—5 μM (Fig. 5C, inset). The linear regression equation was fitted as $A_{522}/A_{656}=0.1239 \times C_{ATP}$ (μM)+0.8367 with a correlation coefficient of 0.9989 (n=10). The limit of detection (LOD) was evaluated to 0.1 μM ATP at $3s_{blank}$ criterion, showing evidence of high sensitivity. The analytical performance of our proposed strategy was comparable to the previously reported aptasensors with colorimetric, fluorescent, chemiluminescent or electrochemical readout (Table S1).

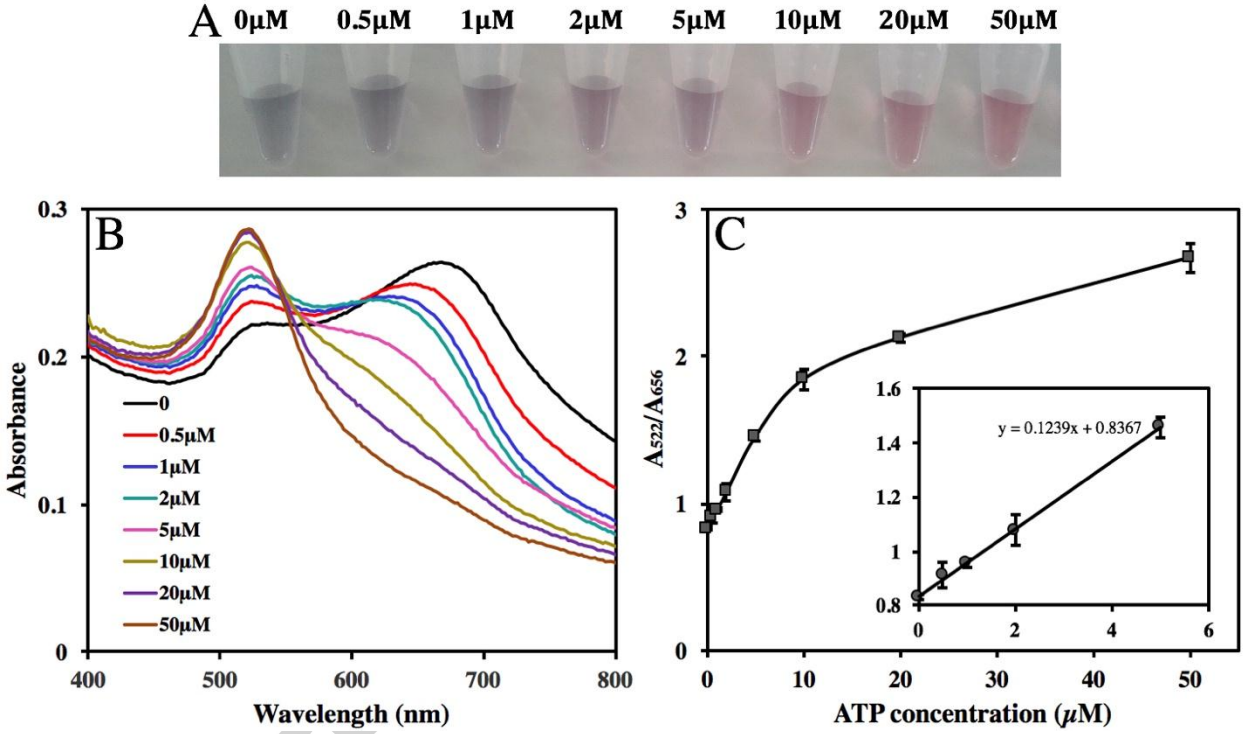

Fig. 5. (A) Color change of AuNPs at different concentrations of ATP. (B) UV–vis absorption spectra following incubation with different ATP concentrations. (C) The absorption ratio (A_{522}/A_{656}) was plotted as a function of ATP concentration. Inset: typical calibration curve for ATP in the 0–5 μM range. Error bars: SD, n=3.

3.5. Selectivity of the Proposed Aptasensor

The selectivity of this aptasensor was examined by challenging this system against other ATP analogs, such as guanosine triphosphate (GTP), uridine triphosphate (UTP), and cytidine triphosphate (CTP) under the optimized conditions. As shown in Fig. 6, only ATP showed a distinctive absorption peak at 522 nm. It was clear that the AuNPs solution could be protected in red color only in the presence of ATP. Conversely, the AuNPs solution appeared blue with ATP analogs (Fig. 6,

inset). All these results suggested that this colorimetric sensing assay is highly selective for ATP.

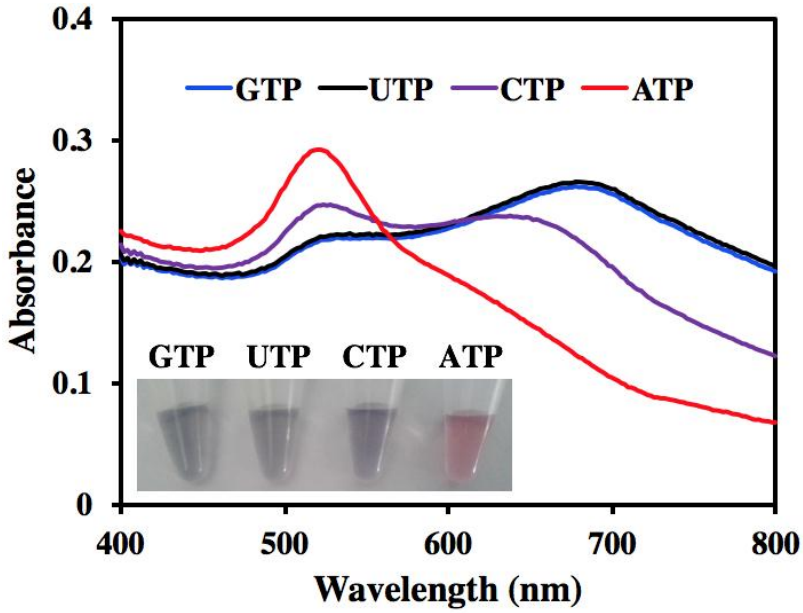

Fig. 6. UV–vis absorption spectra of the colorimetric assay system against GTP (100 μM), UTP (100 μM), CTP (100 μM) and ATP (100 μM), respectively. Inset: visual color changes corresponding to UV–vis absorption spectra.

3.6. Application in Real Sample Detection

To further investigate the feasibility of the proposed colorimetric assay in real biological samples, we tested ATP in complex real samples such as breast cancer cell (MCF-7) lysates. As demonstrated in Fig. 7, the cell lysate (2% diluted and 5% diluted) containing ATP induced the conformational change of AHP and effectively protected the AuNPs from aggregation, corresponding in a red color. In contrast, the blank cell lysate kept AHP untouched, resulting in the obvious aggregation of AuNPs and visually manifesting with a blue color. Our detection performed well in these complex real samples. However, we found that when we increased the concentration of the cell lysate (10% diluted), the large number of non-specific molecules began to affect the detection. We postulated that proteins from the lysate interfered with the read-out. To probe into the possibility, we carried out the proposed colorimetric assay in milk. As illustrated in Figure S1, even 2% diluted milk could affect the detection. This observation indicates that the non-specific adsorption of proteins could protect AuNPs from aggregation, resulting in a high background signal. The results suggest that the proposed colorimetric assay for ATP detection could be used in real sample analysis, although caution needs to be exercised for background signal.

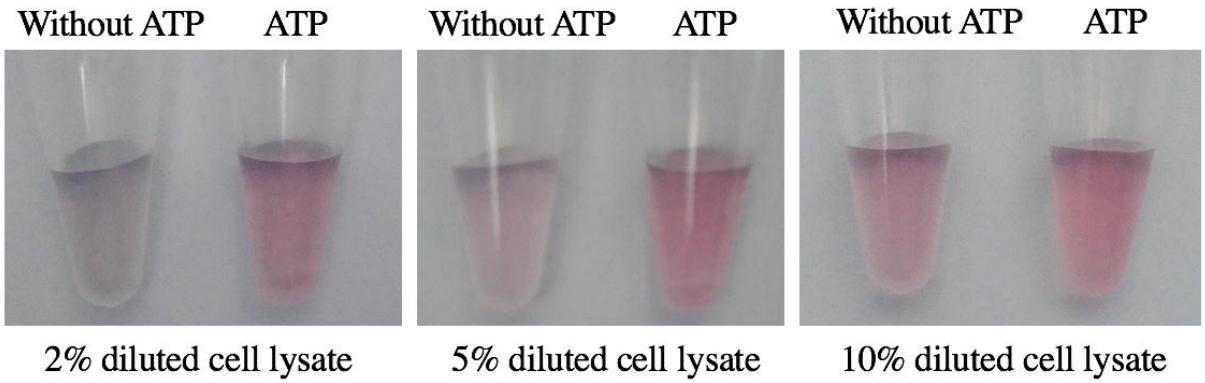

Fig. 7. Our detection performed well in complicated real samples such as 2% diluted cell lysate and 5% diluted cell lysate. When we employed 10% diluted cell lysate, the large number of non-specific molecules began to affect the detection.

4. Conclusion

In summary, we have developed a novel colorimetric aptasensor for rapid and facile detection of ATP by using aptamer-based hairpin probes and unmodified AuNPs. The strategy relies on the excellent specificity of aptamer towards ATP, as well as the different adsorption affinity between aptamer-ATP complex, ssDNA end and AHP towards AuNPs. For probing the target ATP, this assay possessed three excellent advantages. Firstly, it eliminated the need for chemical modifications, complicated separation processes and sophisticated instrumentation, which was simple and cost-effective. Secondly, the assay was rapid in process and convenient for use. It could detect target ATP sensitively and selectively within 5 minutes. Thirdly, this strategy could be applied to analyze other targets with interest by controlling the sequences of the corresponding aptamers, thus representing a universal detection scheme. Moreover, this aptasensor exhibited a good detection performance in real biological samples. With these characteristics, the proposed strategy holds great promise in point-of-care applications.

Acknowledgments

This work was supported by the Ministry of Science and Technology of China (2012ZX09506001-010), and National Natural Science Foundation of China (No. 21302108).

Appendix A. Supporting information

References

[1] A.D. Ellington, J.W. Szostak, In vitro selection of RNA molecules that bind specific ligands, Nature, 346 (1990) 818-822.
[2] C. Tuerk, L. Gold, Systematic evolution of ligands by exponential enrichment: RNA ligands to bacteriophage T4 DNA polymerase, Science, 249 (1990) 505-510.
[3] R. Nutiu, Y. Li, In vitro selection of structure-switching signaling aptamers †, Angewandte Chemie, 44 (2005) 1061-1065.
[4] D.E. Huizenga, J.W. Szostak, A DNA aptamer that binds adenosine and ATP. 34 (1995) 656-665.
[5] H. Ueyama, M. Takagi, S. Takenaka, A novel potassium sensing in aqueous media with a synthetic oligonucleotide derivative. Fluorescence resonance energy transfer associated with Guanine quartet-potassium ion complex formation, Journal of the American Chemical Society, 124 (2002) 379-394.
[6] L.C. Bock, L.C. Griffin, J.A. Latham, E.H. Vermaas, J.J. Toole, Selection of single-stranded DNA molecules that bind and inhibit human thrombin, Nature, 355 (1992) 564-566.
[7] T. Mori, A. Oguro, T. Ohtsu, Y. Nakamura, RNA aptamers selected against the receptor activator of NF-κB acquire general affinity to proteins of the tumor necrosis factor receptor family, Nucleic Acids Research, 32 (2004) 6120-6128.
[8] D. Shangguan, Y. Li, Z. Tang, Z.C. Cao, H.W. Chen, P. Mallikaratchy, K. Sefah, C.J. Yang, W. Tan, Aptamers evolved from live cells as effective molecular probes for cancer study, Proceedings of the National Academy of Sciences of the United States of America, 103 (2006) 11838-11843.
[9] C.L.A. Hamula, H. Zhang, L.L. Guan, X.F. Li, X.C. Le, Selection of aptamers against live bacterial cells, Analytical Chemistry, 80 (2008) 7812-7819.
[10] S. Tombelli, M. Minunni, M. Mascini, Analytical applications of aptamers, Biosensors & Bioelectronics, 20 (2007) 2424-2434.
[11] I. Willner, M. Zayats, Electronic aptamer-based sensors, Angewandte Chemie International Edition, 46 (2007) 6408-6418.
[12] W. Zhou, P.J. Huang, J. Ding, J. Liu, Aptamer-based biosensors for biomedical diagnostics, Analyst, 139 (2014) 2627-2640.
[13] J. Das, K.B. Cederquist, A.A. Zaragoza, P.E. Lee, E.H. Sargent, S.O. Kelley, An ultrasensitive universal detector based on neutralizer displacement, Nature Chemistry, 4 (2012) 642-648.
[14] Y. He, Z.G. Wang, H.W. Tang, D.W. Pang, Low background signal platform for the detection of ATP: when a molecular aptamer beacon meets graphene oxide, Biosensors & Bioelectronics, 29 (2011) 76-81.
[15] L. Kong, J. Xu, Y. Xu, Y. Xiang, R. Yuan, Y. Chai, A universal and label-free aptasensor for fluorescent detection of ATP and thrombin based on SYBR Green I dye, Biosensors & Bioelectronics, 42 (2013) 193-197.
[16] Y. Wei, Y. Chen, H. Li, S. Shuang, C. Dong, G. Wang, An exonuclease I-based label-free fluorometric aptasensor for adenosine triphosphate (ATP) detection with a wide concentration range, Biosensors & Bioelectronics, 63 (2015) 311-316.
[17] Y. He, J. Tian, K. Hu, J. Zhang, S. Chen, Y. Jiang, Y. Zhao, S. Zhao, An ultrasensitive quantum dots fluorescent polarization immunoassay based on the antibody modified Au nanoparticles amplifying for the detection of adenosine triphosphate, Analytica Chimica Acta, 802 (2013) 67-73.

[18] Q. Chen, Q. Guo, Y. Chen, J. Pang, F. Fu, L. Guo, An enzyme-free and label-free fluorescent biosensor for small molecules by G-quadruplex based hybridization chain reaction, Talanta, 138 (2015) 15-19.
[19] Z. Liu, S. Chen, B. Liu, J. Wu, Y. Zhou, L. He, J. Ding, J. Liu, Intracellular detection of ATP using an aptamer beacon covalently linked to graphene oxide resisting nonspecific probe displacement, Analytical Chemistry, 86 (2014) 12229-12235.
[20] H. Zhang, B. Jiang, X. Yun, Y. Zhang, Y. Chai, R. Yuan, Aptamer/quantum dot-based simultaneous electrochemical detection of multiple small molecules, Analytica Chimica Acta, 688 (2011) 99-103.
[21] X. Zuo, S. Song, J. Zhang, D. Pan, L. Wang, C. Fan, A target-responsive electrochemical aptamer switch (TREAS) for reagentless detection of nanomolar ATP, Journal of the American Chemical Society, 129 (2007) 1042-1043.
[22] Y. Mao, J. Liu, D. He, X. He, K. Wang, H. Shi, L. Wen, Aptamer/target binding-induced triple helix forming for signal-on electrochemical biosensing, Talanta, 143 (2015) 381-387.
[23] Q. Zhou, Y. Lin, Y. Lin, Q. Wei, G. Chen, D. Tang, In situ amplified electrochemical aptasensing for sensitive detection of adenosine triphosphate by coupling target-induced hybridization chain reaction with the assembly of silver nanotags, Talanta, 146 (2016) 23-28.
[24] Z.M. Zhou, Y. Yu, Y.D. Zhao, A new strategy for the detection of adenosine triphosphate by aptamer/quantum dot biosensor based on chemiluminescence resonance energy transfer, Analyst, 137 (2012) 4262-4266.
[25] X. Liu, R. Freeman, E. Golub, I. Willner, Chemiluminescence and chemiluminescence resonance energy transfer (CRET) aptamer sensors using catalytic hemin/G-quadruplexes, Acs Nano, 5 (2011) 7648-7655.
[26] Y. Li, X. Ji, W. Song, Y. Guo, Design of a sensitive aptasensor based on magnetic microbeads-assisted strand displacement amplification and target recycling, Analytica Chimica Acta, 770 (2013) 147-152.
[27] J. Li, H.E. Fu, L.J. Wu, A.X. Zheng, G.N. Chen, H.H. Yang, General colorimetric detection of proteins and small molecules based on cyclic enzymatic signal amplification and hairpin aptamer probe, Analytical Chemistry, 84 (2012) 5309-5315.
[28] D. Cheng, Y. Li, J. Wang, Y. Sun, L. Jin, C. Li, Y. Lu, Fluorescence and colorimetric detection of ATP based on a strategy of self-promoting aggregation of a water-soluble polythiophene derivative, Chemical Communications, 51 (2015) 8544-8546.
[29] Y. Huo, L. Qi, X.J. Lv, T. Lai, J. Zhang, Z.Q. Zhang, A sensitive aptasensor for colorimetric detection of adenosine triphosphate based on the protective effect of ATP-aptamer complexes on unmodified gold nanoparticles, Biosensors & Bioelectronics, 78 (2016) 315-320.
[30] S. Cheng, B. Zheng, M. Wang, M.H. Lam, X. Ge, Double-functionalized gold nanoparticles with split aptamer for the detection of adenosine triphosphate, Talanta, 115 (2013) 506-511.
[31] Y. Helwa, N. Dave, R. Froidevaux, A. Samadi, J. Liu, Aptamer-functionalized hydrogel microparticles for fast visual detection of mercury(II) and adenosine, Acs Applied Materials & Interfaces, 4 (2012) 2228-2233.
[32] J. Zhang, L. Wang, D. Pan, S. Song, F.Y. Boey, H. Zhang, C. Fan, Visual cocaine detection with gold nanoparticles and rationally engineered aptamer structures, Small, 4 (2008) 1196-1200.

[33] B. Zou, X. Cao, H. Wu, Q. Song, J. Wang, T. Kajiyama, H. Kambara, G. Zhou, Sensitive and specific colorimetric DNA detection by invasive reaction coupled with nicking endonuclease-assisted nanoparticles amplification, Biosensors & Bioelectronics, 66 (2015) 50-54.
[34] F. Su, L. Wang, Y. Sun, C. Liu, X. Duan, Z. Li, Highly sensitive detection of CpG methylation in genomic DNA by AuNP-based colorimetric assay with ligase chain reaction, Chemical Communications, 51 (2015) 3371-3374.
[35] W. Zhao, W. Chiuman, J.C. Lam, S.A. Mcmanus, W. Chen, Y. Cui, R. Pelton, M.A. Brook, Y. Li, DNA aptamer folding on gold nanoparticles: from colloid chemistry to biosensors, Journal of the American Chemical Society, 130 (2008) 3610-3618.
[36] C.A. Mirkin, R.L. Letsinger, R.C. Mucic, J.J. Storhoff, A DNA-based method for rationally assembling nanoparticles into macroscopic materials, Nature, 382 (1996) 607-609.
[37] Y.W.C. Cao, R. Jin, C.A. Mirkin, Nanoparticles with Raman spectroscopic fingerprints for DNA and RNA detection, Science, 297 (2002) 1536-1540.
[38] J. Liu, Y. Lu, Non-base pairing DNA provides a new dimension for controlling aptamer-linked nanoparticles and sensors, Journal of the American Chemical Society, 129 (2007) 8634-8643.
[39] H. Li, L. Rothberg, Colorimetric detection of DNA sequences based on electrostatic interactions with unmodified gold nanoparticles, Proceedings of the National Academy of Sciences of the United States of America, 101 (2004) 14036-14039.
[40] H. Wang, Y. Wang, J. Jin, R. Yang, Gold nanoparticle-based colorimetric and “turn-on” fluorescent probe for mercury(II) ions in aqueous solution, Analytical Chemistry, 80 (2009) 9021-9028.
[41] K. Ai, Y. Liu, L. Lu, Hydrogen-bonding recognition-induced color change of gold nanoparticles for visual detection of melamine in raw milk and infant formula, Journal of the American Chemical Society, 131 (2009) 9496-9497.
[42] H. Wei, B. Li, J. Li, E. Wang, S. Dong, Simple and sensitive aptamer-based colorimetric sensing of protein using unmodified gold nanoparticle probes, Chemical Communications, 36 (2007) 3735-3737.
[43] P. Liu, X. Yang, S. Sun, Q. Wang, K. Wang, J. Huang, J. Liu, L. He, Enzyme-free colorimetric detection of DNA by using gold nanoparticles and hybridization chain reaction amplification, Analytical Chemistry, 85 (2013) 7689-7695.
[44] M. Zhang, G. Qing, C. Xiong, R. Cui, D.W. Pang, T. Sun, Dual-responsive gold nanoparticles for colorimetric recognition and testing of carbohydrates with a dispersion-dominated chromogenic process, Advanced Materials, 25 (2013) 749-754.
[45] F. Xia, X. Zuo, R. Yang, Y. Xiao, D. Kang, A. Valléebélisle, X. Gong, J.D. Yuen, B.B. Hsu, A.J. Heeger, Colorimetric detection of DNA, small molecules, proteins, and ions using unmodified gold nanoparticles and conjugated polyelectrolytes, Proceedings of the National Academy of Sciences, 107 (2010) 10837-10841.
[46] L. Wu, X. Zhang, W. Liu, E. Xiong, J. Chen, Sensitive electrochemical aptasensor by coupling “signal-on’’ and “signal-off’’ strategies, Analytical Chemistry, 85 (2013) 8397-8402.
[47] J.M. Berg, J.L. Tymoczko, L. Stryer, Biochemistry 5th ed, (2002).
[48] H. Yokoshiki, M. Sunagawa, T. Seki, N. Sperelakis, ATP-sensitive K+ channels in pancreatic, cardiac, and vascular smooth muscle cells, American Journal of Physiology, 274 (1998) 25-37.

[49] Z. Zhou, Y. Du, S. Dong, Double-strand DNA-templated formation of copper nanoparticles as fluorescent probe for label-free aptamer sensor, Analytical Chemistry, 83 (2011) 5122-5127.
[50] Y. Ma, S. Adjemian, H. Yang, J.P. Catani, D. Hannani, I. Martins, M. Michaud, O. Kepp, A.Q. Sukkurwala, E. Vacchelli, ATP-dependent recruitment, survival and differentiation of dendritic cell precursors in the tumor bed after anticancer chemotherapy, Oncoimmunology, 2 (2013) e24568-e24568.
[51] K.C. Grabar, R.G. Freeman, M.B. Hommer, M.J. Natan, Preparation and characterization of Au colloid monolayers, Analytical Chemistry, 67 (1995) 735-743.
[52] W. Haiss, N.T. Thanh, J. Aveyard, D.G. Fernig, Determination of size and concentration of gold nanoparticles from UV-vis spectra, Analytical Chemistry, 79 (2007) 4215-4221.

Highlights

- The detection time was significantly decreased to 5 minutes.
- The colorimetric aptasensor presented a high sensitivity and specificity for target ATP.
- The aptasensor can be applied to perform assay in real samples.